

## Numerical Modeling of Flow into Primary Dedusting System of a 130t Converter

Breno Totti Maia  
Lumar Metals  
Rod. MG 232 km09 n°100  
Santana do Paraíso – Minas Gerais, Brazil ZIP Code:35.162-970  
Phone – +55 31 9399 3200  
E-mail: [breno.totti@lumarmetals.com.br](mailto:breno.totti@lumarmetals.com.br)

Bruno Orlando de Almeida Santos  
Lumar Metals  
Rod. MG 232 km09 n°100  
Santana do Paraíso – Minas Gerais, Brazil ZIP Code:35.162-970  
Phone – +55 31 9399-3534  
E-mail: [bruno.santos@lumarmetals.com.br](mailto:bruno.santos@lumarmetals.com.br)

Fabrcício Silveira Garajau  
Lumar Metals  
Rod. MG 232 km09 n°100  
Santana do Paraíso – Minas Gerais, Brazil ZIP Code:35.162-970  
Phone – +55 31 9399-3337  
E-mail: [fabricao.garajau@lumarmetals.com.br](mailto:fabricao.garajau@lumarmetals.com.br)

Hugo Leonardo de Freitas  
Arcelor Mittal João Monlevade  
Av. Getúlio Vargas, 100, Centro Industrial  
João Monlevade - Minas Gerais, Brazil ZIP code: 3.5930-395  
Phone – +55 31 8634 2358  
E-mail: [hugo.freitas@arcelormittal.com.br](mailto:hugo.freitas@arcelormittal.com.br)

Jose Geraldo Torres  
Arcelor Mittal João Monlevade  
Av. Getúlio Vargas, 100, Centro Industrial  
João Monlevade - Minas Gerais, Brazil ZIP code: 3.5930-395  
Phone – +55 31 8634 2358  
E-mail: [jose.torres@arcelormittal.com.br](mailto:jose.torres@arcelormittal.com.br)

Marcelo de Souza Lima Guerra  
Lumar Metals  
Rod. MG 232 km09 n°100  
Santana do Paraíso – Minas Gerais, Brazil ZIP Code:35.162-970  
Phone – +55 31 8788 4981  
E-mail: [marcelo.guerra@lumarmetals.com.br](mailto:marcelo.guerra@lumarmetals.com.br)

Roberto Parreiras Tavares  
Universidade Federal de Minas Gerais (UFMG)  
Av. Antônio Carlos, 6627, Pampulha  
Belo Horizonte, Minas Gerais, Brazil ZIP Code: 31.270-901  
Phone – +55 31 3409-1806  
E-mail: [rtavares@demet.ufmg.br](mailto:rtavares@demet.ufmg.br)

Rudolf Huebner  
Universidade Federal de Minas Gerais (UFMG)  
Av. Antônio Carlos, 6627, Pampulha  
Belo Horizonte, Minas Gerais, Brazil ZIP Code: 31.270-901  
Phone – +55 31 3409-1806  
E-mail: [rudolf@ufmg.br](mailto:rudolf@ufmg.br)

Key words: Dedusting system, CFD, Temperature, Duct geometry

## INTRODUCTION

The dedusting system is a device to control air pollution that function is to take, flow gases and fine solids. The other function is to split solids of the gases. There are two mainly types: dry systems and wet systems. In this study, the 130t LD converter has these two types. The primary dedusting is the wet system and used to take the gases direct from the converter's mouth. The secondary dedusting is the dry system and collect fumes around converter.

The primary dedusting is responsible to collect fumes that come from the oxygen blown into the metallic bath, sometime the secondary system is responsible to collect fumes from the charge hot metal and scrap into converter and fugitives gases and fumes during blow.

In the wet systems, the gases are partially cooling by the cooling ducts. The next stages: quencher and venturi system is important to separate the solids particles from de gas flow. After quencher is removed hard washed of the fumes and the venturi is a fine washed with the aim to obey the environmental law.

The fumes blow up from converter with high temperature around 1700oC. The solid part has high content of the FeO, CaO, C and other slag elements. These fumes enter into duct together with air. The amount of air depends of the kind of the skirt that determine the suppress combustion when the skirt is movable or complete combustion when the skirt is fixed.

The hood and cooling stack are made with bundle of pipes welded together. Water circulates into the pipes to absorb the radiation and convection heat from gases by pipe's wall. The mainly function of the heat transfer for pipes is reduce temperature, and by this way, reduce the volume of fumes

During the passage of fumes into dedusting system, the contacts with cooling pipes promote convection in wall pipes. The efficiency is a function the correct water flow, water temperature control in the system inlet and outlet, pressure and back pressure in the circuit and water control quality. For the other side, the correct dimension duct and pipes guarantee correct residence time of fumes with adequate contact fume-wall pipe, maximizing heat transfer.

The cooling water is pumped to system by closed and pressurized circuit. The heat is removed from the gases and dissipated with the air through heat exchanger. The circuit has tanks pressurized wit nitrogen to obtain constant pressure and increase boiling temperature of water and permit to extract more heat form the system.

The gases, before to clean, needs to reduce temperature until around 900°C by the hood and cooling stack.

The exhaustion capacity is determined by fan capacity and respective system pressure drop. It is very important some excess in fan capacity to consider some operation deviation.

Other important factor in this first stage of the wet dedusting system is a ducts geometry criteria's. The aim is an uniform flow of fumes during the cooling duct.

The numerical calculations from computational methods are tools that allow analyses of parameters described with the possibilities to identify device problems in the project stage or during operation. It is a stronger tool to help maintenance people is the reason of problems and developed the best solution.

## MODEL FORMULATION GOVERNING EQUATION FOR GAS

The gas phase is described by transport equations of the continuous phase, being the Navier-Stokes equations solved by conservative form. The equations solved to gas phase include mass conservation, momentum, turbulent kinetic energy, rate of turbulent dissipation, enthalpy and chemical species. The mass conservation and momentum equations are:

$$\frac{\partial \rho}{\partial t} + \nabla \cdot (\rho \vec{U}) = S_m \quad (1)$$

$$\frac{\partial}{\partial t} (\rho v) + \nabla \cdot (\rho \vec{U} \vec{U}) = -\nabla p + \nabla \cdot (\vec{\tau}) + \rho \vec{g} + \vec{F} \quad (2)$$

Where  $\rho$  is gas density,  $U$  velocity and term  $S_m$  is mass added in the continuous phase by the second disperse phase. The  $p$  term is static pressure,  $\vec{\tau}$  stress tensor and  $\rho \vec{g}$  and  $\vec{F}$  are gravitational forces of body and external forces respectively.

The energy equation is derivate of the first thermodynamics law that the rate energy variation of one particle of fluid is equal the rate heat to one particle of fluid added work made. For the steady stationary, the energy equation is solved like show:

$$\frac{\partial (\rho h_{tot})}{\partial t} - \frac{\partial p}{\partial t} + \nabla \cdot (\rho v h_{tot}) - \nabla \cdot (k \nabla T) + \nabla \cdot (v \cdot \tau) + v \cdot S_M + S_E \quad (3)$$

Where  $\nabla \cdot (v \tau)$  term represent work by viscous tensions and  $v \cdot S_M$  is work by external momentum forces, being normally neglected. The  $h_{tot}$  term is total enthalpy related with the static enthalpy  $h(T, p)$  by equation:

$$h_{tot} = h + \frac{1}{2}v^2 \quad (4)$$

The mixer model and chemical species transport are based in conservations equations that describe convection and diffusion sources and reactions for each chemical species. To solve the conservation equations is foreseen a region for each chemical specie  $Y_i$  through solution of the convection/diffusion equation for each chemical specie, that show basic form like the equation below.

$$\frac{\partial}{\partial t}(\rho Y_i) + \nabla \cdot (\rho \vec{v} Y_i) = -\nabla \cdot \vec{J}_i + R_i + S_i \quad (5)$$

Where  $R_i$  is production rate of one chemical specie  $i$ . The reaction is calculated like the sum of reaction Arrhenius source over number of reactions that specie run, showed in equation. The term  $J_i$  is diffusive flow of species  $i$ , that appears form gradients concentration and temperature.

$$R_i = M_{w,i} \sum_{r=1}^{N_R} \tilde{R}_{i,r} \quad (6)$$

Turbulence model  $k$ - $\varepsilon$  is based on model of transport equations to kinetic energy of turbulence ( $k$ ), defined like variations in the velocity fluctuations, and the rate turbulence dissipation ( $\varepsilon$ ), defined like the rate which occurs the dissipation in the velocity fluctuations. This model introduce two new variables in the system of equations, being based in turbulent viscous concept  $\mu_t$ , assume that the turbulent viscous is linked with kinetic turbulent energy and dissipation, like show the equation

$$\mu_t = C_\mu \rho \frac{k^2}{\varepsilon} \quad (7)$$

The values of  $k$  and  $\varepsilon$  are obtained for differential equations of transport, like the equations:

$$\frac{\partial(\rho k)}{\partial t} + \frac{\partial}{\partial x_j}(\rho U_j k) = \frac{\partial}{\partial x_j} \left[ \left( \mu + \frac{\mu_t}{\sigma_k} \right) \frac{\partial k}{\partial x_j} \right] + P_k - \rho \varepsilon + P_{kb} \quad (8)$$

$$\frac{\partial(\rho \varepsilon)}{\partial t} + \frac{\partial}{\partial x_j}(\rho U_j \varepsilon) = \frac{\partial}{\partial x_j} \left[ \left( \mu + \frac{\mu_t}{\sigma_\varepsilon} \right) \frac{\partial \varepsilon}{\partial x_j} \right] + \frac{\varepsilon}{k} (C_{\varepsilon 1} P_k - C_{\varepsilon 2} \rho \varepsilon + C_{\varepsilon 1} P_{\varepsilon b}) \quad (9)$$

In these equations  $C_\mu$ ,  $C_{\varepsilon 1}$ ,  $C_{\varepsilon 2}$ ,  $\sigma_k$  and  $\sigma_\varepsilon$  are constants of turbulence model. Now,  $P_{kb}$  and  $P_{\varepsilon b}$  represent flutuability forces and  $P_k$  is production of turbulence due viscous forces.

## PARTICLE GOVERNING EQUATION

The forces that act in particle travel through fluid affect your acceleration due difference between velocities of particle and fluid, as well fluid dislocations over the particle. The movement equation for this particle, considering all force acting in the system was derivate by researches Basset, Boussinesq and Oseen, and showed for the equation.

$$m_p \frac{dv_p}{dt} = F_D + F_B + F_R + F_{VM} + F_P + F_{BA} \quad (10)$$

Where  $F_D$  represents drag forces act in particle,  $F_B$  is a flutuability forces due gravity,  $F_R$  are rotation domain forces, represents mass force added, or virtual,  $F_P$  gradient pressure forces and  $F_{BA}$  is knowed like Basset term, that represents deviation in the standard flow. The change rate of temperature is commanded for three physical processes: convective heat transfer, mass transfer and radiation. The change rate of temperature in particle is obtained for sum like the equation:

$$\sum (m_C C_P) \frac{dT}{dt} = Q_C + Q_M + Q_R \quad (11)$$

Where  $Q_C$ ,  $Q_M$  and  $Q_R$  are heats transfers for convection, mass and radiation.

The instantaneous velocity calculations of fluid,  $v_f$  depends of flow regime and kind of particles. For turbulence regime, the instantaneous velocity of fluid is decomposed in principal component  $v_f$  and fluctuant  $v'_f$ . The turbulent dispersion of particle is model assumed that each particle is into single turbulent swirl, being each swirl has fluctuant velocity,  $v'_f$  duration,  $\tau_\varepsilon$ , and characteristic length,  $l_\varepsilon$ , calculated by Gosman and Ioannides, and showed for the equations.

$$v'_f = \Gamma(2k/3)^{0.5} \quad (12)$$

$$\tau_e = \frac{l_e}{\left(\frac{2k}{3}\right)^{\frac{1}{2}}} \quad (13)$$

$$l_e = \frac{C_\mu^{\frac{3}{4}} k^{\frac{3}{2}}}{\varepsilon} \quad (14)$$

Where  $C_\mu$  is turbulence constant.

The aerodynamics drag force  $F_D$  over particle is proportional the flow velocity  $U$ , between fluid and particle, like equation.

$$F_D = \frac{1}{2} C_D \rho_F A_F (U_F - U_P) \quad (15)$$

Where  $CD$  is drag coefficient,  $A_F$  is effective transversal particle section,  $U_F$  and  $U_P$  are velocities of fluid and particle, respectively.

$$C_D = \max\left[\frac{24}{Re}(1 + 0,15 Re^{0,687}); 0,44\right] \quad (16)$$

Now, buoyant force over particle is force acting in particle immerse into fluid, and can be described like equation.

$$F_B = \frac{\pi}{6} d_p^3 (\rho_p - \rho_f) g \quad (17)$$

Where  $d_p$  is particle diameter,  $\rho_p$  is particle density,  $\rho_f$  fluid density and  $g$  gravity vector.

## CO COMBUSTION

During converter operation some amounts of environmental air enter by skirt. The oxygen of this air reacts with carbon monoxide came from the furnace. This combustion model use transport equation to mass fraction for the component  $Y_i$ .

$$\frac{\partial(\rho Y_i)}{\partial t} + \frac{\partial(\rho U_j Y_i)}{\partial x_j} = \frac{\partial}{\partial x_j} \left( \Gamma_{ie,f} \frac{\partial Y_i}{\partial x_j} \right) + S_i \quad (18)$$

Where source term  $S_i$  refers the rate of chemical reaction involved  $i$  component. Generally, the rate of production and consumption of  $S_i$  to  $i$  component can be computed how sum of progress rates for all elementary reactions which  $i$  participates, like the equation

$$S_i = W_i \sum_{n=1}^N (v_{ni}'' - v_{ni}') R_n \quad (19)$$

Where  $v_{ni}$  is stoichiometric coefficient to  $i$  component in the elementary reaction  $n$ ,  $R_n$  is a rate of elementary reaction to the reaction  $n$ .

## MATERIAL AND METHODS MODELING DEDUSTING SYSTEM

The computational analysis for the dedusting system was shared in four parts. The first simulation is based in same data about device actually in operation. The second simulation the inner diameter was increased, for 2200mm. Change in joints was introduced in third simulation, being big change the curve located on the top of the system. The joints are softening. The fourth option was made a extrapolation of dimensions to 2900mm, showed in Figure 1.

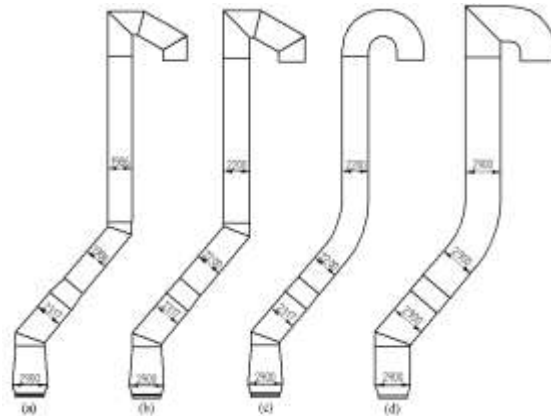


Figure 1 – Dedusting system dimensions, (a) actual, (b) change 1, (c) change 2, smoothing and (d) change 4, extrapolation of the dimensions.

For a good approximation of the results with the information's collected in the operational area, was used an adaptation for the geometry by a no-structured mesh. This mesh is favorable to follow particle through Lagrangian description, individual following of particle considering gravity, drag's forces and turbulent dissipation. A mesh with 400 thousand nodes, showed in figure 2 was used in the computational simulation.

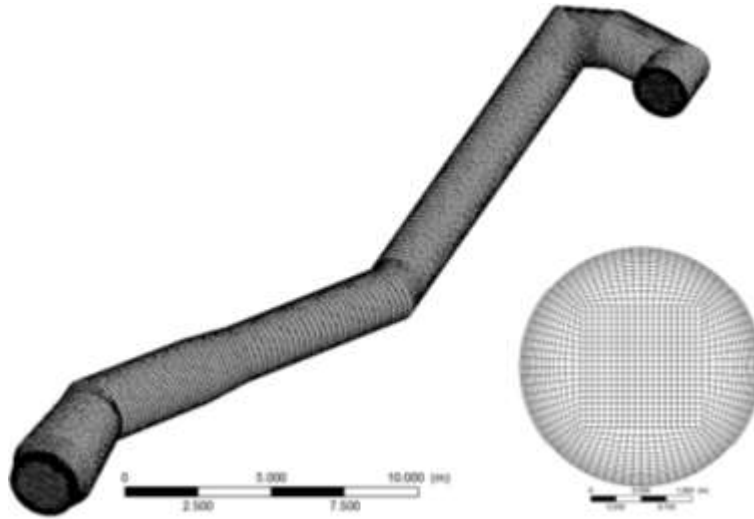


Figure 2 – Computational mesh with 400 thousand nodes and inlet detail.

The boundary conditions were adjusted with parameters collected from operational area. In these simulations were considered two different heights for the skirt: completely closed to the converter mouth and with 100mm above it. A secondary simulation was made for the cooling pipe system. Through this simulation was obtained the equation that describe the behavior of the internal wall temperature, responsible for cooling fumes like a function of internal velocity, showed below

$$T = \left( \frac{T_{min} - T_{max}}{L} \right) X + T_{max} \quad (20)$$

Where  $T_{max}$  is maximum temperature in the wall,  $T_{min}$  is the minimum temperature;  $L$  is the total length of cooling stack and  $X$  Cartesian position. In the enter of system was used a gas flow of 3660 Nm<sup>3</sup>/min , temperature of 1700°C. The pressure in exit the cooling pipes was established in 2500 mmWC.

For simulation with the skirt completely closed any air enters in the hood, just fume flow through dedusting system. When the skirt is open, the air conditions are pressure in 1 atm and temperature 40°C. Table 1 showed the mainly data used in simulations. In the combustion was used factor of flammability equal 0,42. This factor limits stoichiometric of equations and promote adjusts in flame temperature.

Table 1 – Boundary Conditions

	Units	Close skirt	skirt 100mm open
Gas Flow	[Nm <sup>3</sup> /min]	3660	3660
Particles Flow	[kg/s]	1,69	1,69
Ø Particles	[µm]	100	100
Gas Temperatures	[°C]	1700	1700
Enter pressure	[atm]	1	1
Enviromental temperature	[°C]	-	40
Exit pressure	[mmCA]	2500	2500
Water temperature	[°C]	80	80
Pipes roughness	[µm]	0,045	0,045

## RESULTS AND DISCUSSIONS

The results will be show consider first, the skirt completely closed and the second part with open 100mm.

### FLOW WITH THE SKIRT COMPLETELY CLOSED

The results of profile temperature variation across the ducts and top of the dedusting system with skirt completely closed have the same behavior, showed in figure 3.

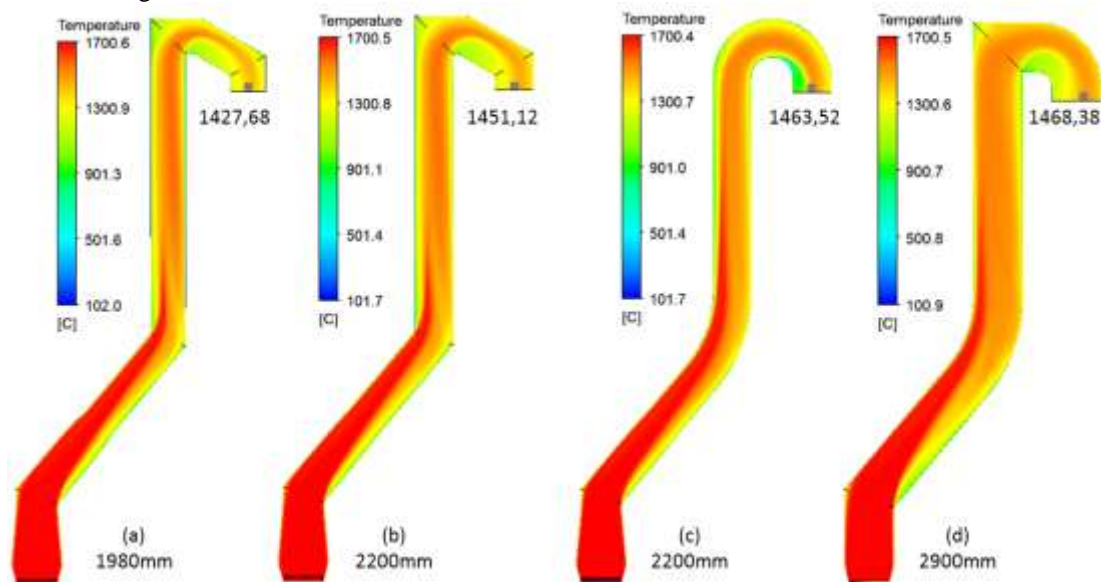


Figure 3 – Temperature profile with different diameters and shape of ducts.

For the same opening condition, energy source programmed in the CFD was equal to four cases. It is necessary to close the balances and convergence. The temperature profile has small variations as function of the geometry, but there is compensation: when duct diameter increase, fume velocity decrease for the same exhaust capacity of the fan. By the fume convective heat transfer coefficient, when the fume velocity decrease, decrease too the convective power, and the impact is under cooling capacity. For system completely closed, the end top temperature has small variations.

In operational practice, the skirt completely closed doesn't occur. Little air infiltrations take place and oxygen reacts with carbon monoxide producing carbon dioxide, for the other side, nitrogen, inert gas with high concentration in the air, promote reduction in fume temperature.

Still in figure 3, fluid flow cause alterations in temperatures yields, proved that special care is necessary for cooling in the hood, skirt movable and first 45° curve.

The inner diameter has strong influence in the flow velocity for the system completely closed. The figure 4 show different velocity profiles along the cooling system. It is possible to see in figure 4 (a), the fast tapering in the inner diameter causes the fume velocity increasing. The high fume velocity has bad consequences in 180° curve at top that accelerate pipes wear. When the inner diameter grow, like in figure 4 (b), average velocity comes down considerably and reduce turbulence in 180° curve at top.

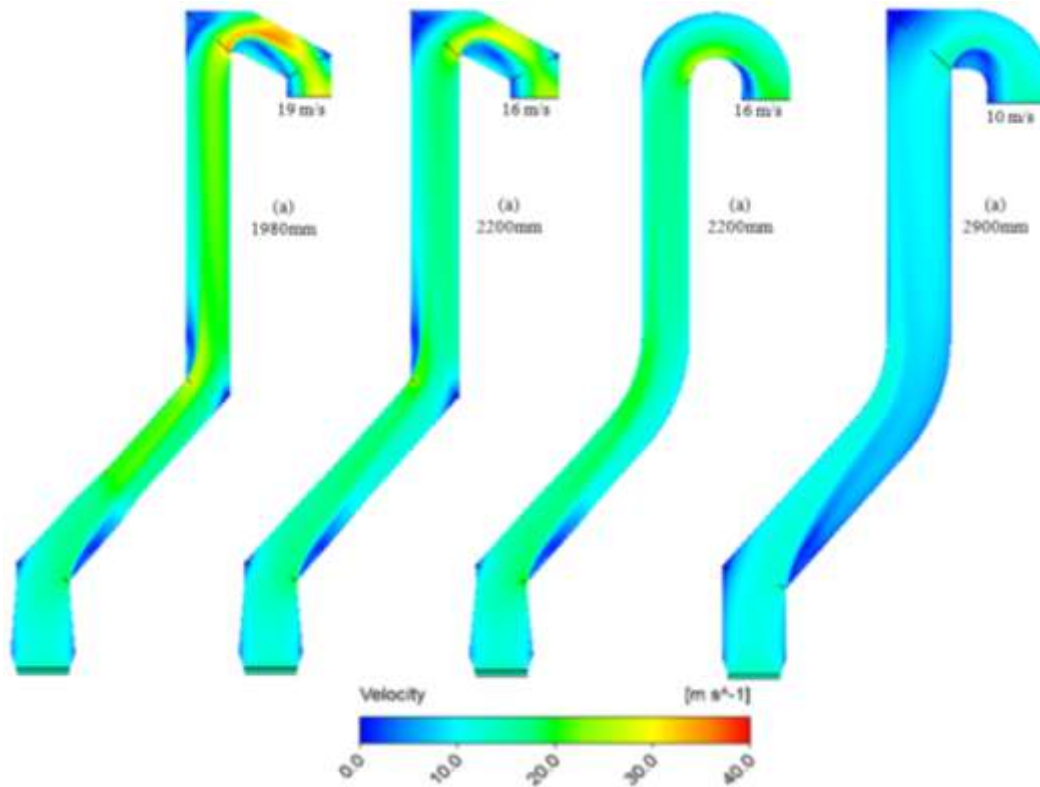


Figure 4 – Velocity profile.

The bigger difference between velocity profiles is due 180° curve at top, When a smooth curve is developed, it is possible to see in figure 4 (c), that velocity in curve reduce significantly when compared with cases (a) and (b). This profile was conceived to have the same direction of the flow reducing the piston volume created for the curve and made a smooth transition for fumes to start clean stage. In figure 4 (d), the extrapolation case shows the ideal situation to obtain good life for the cooling pipes, low average velocity and well distributed along the section that permit good conditions for first stage to clean gas. The figure 5 shows a section of duct in 25m of height.

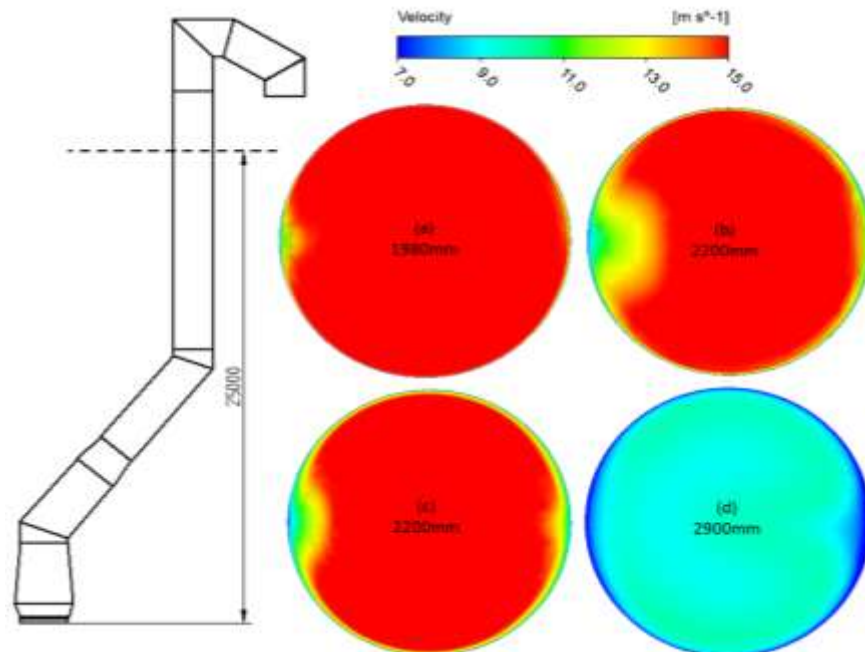


Figure 5- Velocity profile in section 25m above the mouth converter.

It is possible to see that the fume with high velocity has a strong contact with the pipe wall. When the diameter increase and smooth geometry is applied, the velocity near the pipe wall reduces. It is good for pipe lifetime, but it isn't so good for heat transfer.

The fume velocity has stronger influence on particle impact under wall pipe surface. The gas flow drags the particle all the way through the system and as the gas velocity decreases, also decrease the velocity of the dragged particles. The figure 6 show the particles way monitored by Lagrangian discretization method. For the constant flow of particles equal for all simulations, it is possible to observe the same impact region, but the impact intensity is related to the particles velocity impact.

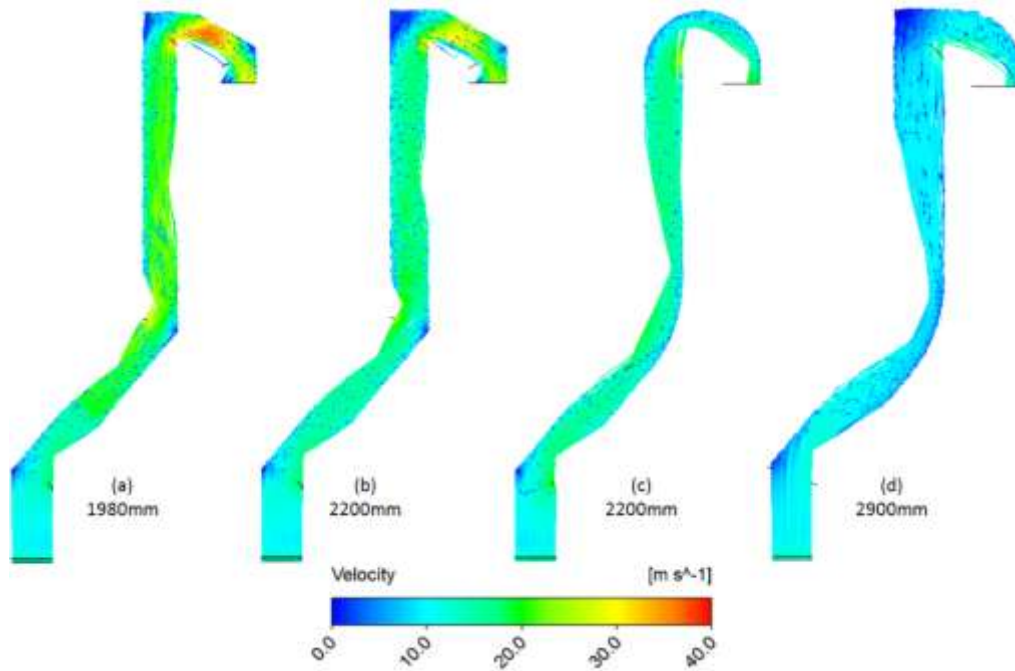


Figure 6 – Particle velocity along dedusting system.

In figure 7, show the particle impact effect under surface of pipe walls in 180° curve. When the curve is smooth, the impact region is less intensive than others. Increasing the inner diameter has the same influence.

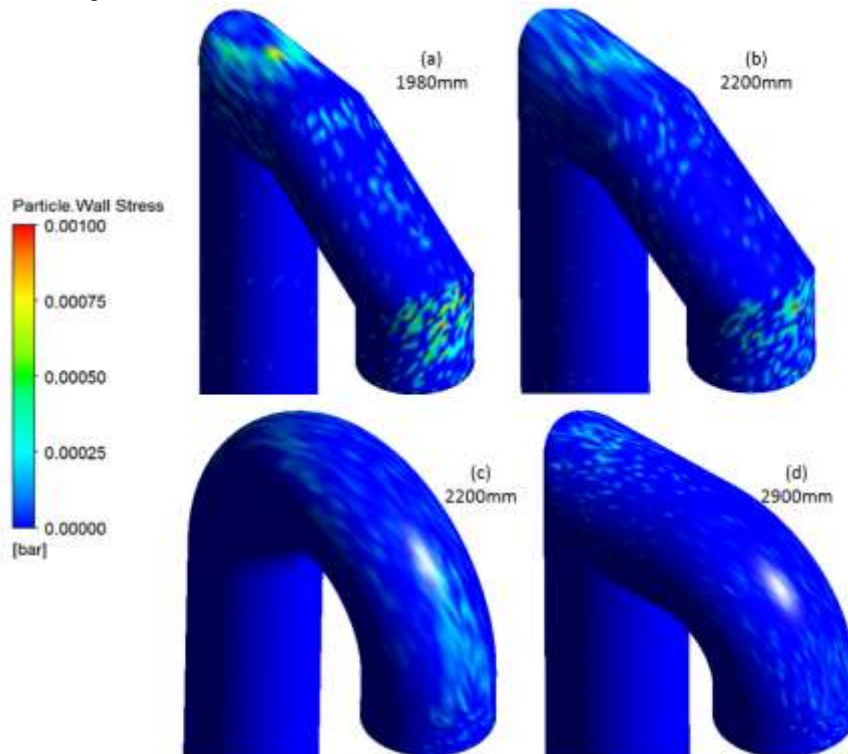


Figure 7 – Particle impact effect under surface of pipe walls.



The profile (c) has the same diameter that profile (b) with 2200mm. The difference in wall pressure is clear in the region where it is necessary to change the flow direction and reduce with smooth geometry. The profile (c) is the best design situation analyzed.

### FLOW WITH OPEN SKIRT

When the skirt is open air admission occurs into the hood. This air starts combustion along the cooling ducts and modifying gas chemical composition and temperature, as shown in figure 8.

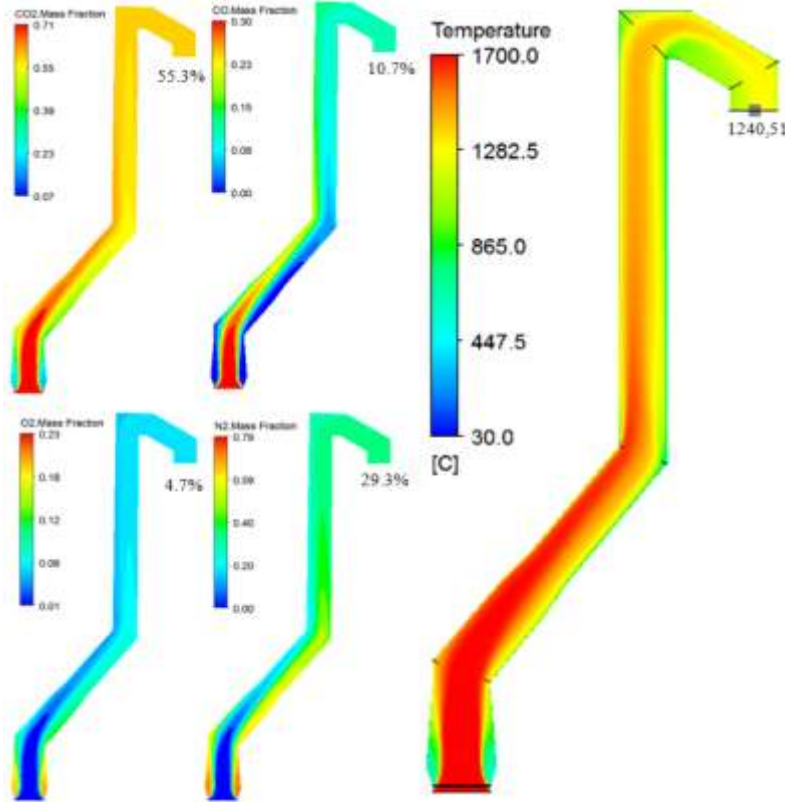


Figure 8 – Gas composition during combustion along the cooling ducts.

The entrance air density is higher than the converter fumes forcing them to the center of the cooling stack. The air reacts with carbon monoxide, increasing the carbon dioxide concentration and temperature along the ducts. The simulation results were verified with industry real values during maximum decarburization time, indicating the compatibility between the CFD study and the real situation.

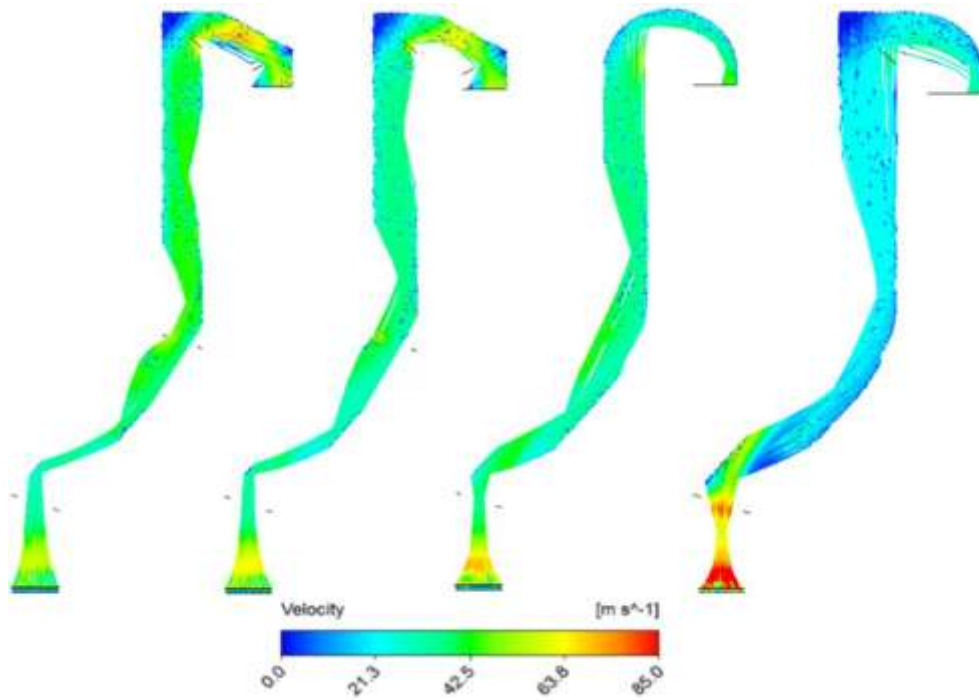


Figure 9 – Particles trajectory along cooling ducts.

Compared figure 9 and figure 6, it is possible to observe that the entrance air forced the fumes to the center resulting in a cone shape. With the change in duct slope and the gas flow centralization, the collision of particles is enhanced in specific regions of the hood and highlighted in Figure 10.

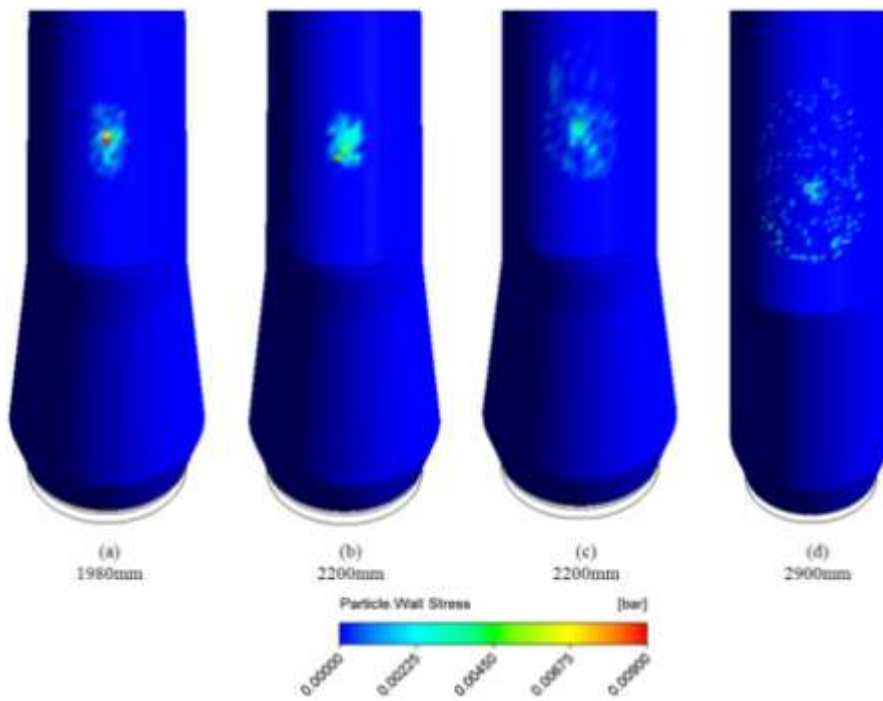


Figure 11 – Particle impact in the first curve of dedusting system.

The particles impact of the particles is also motivated by high temperature in the same region. The results of this analysis coincide with the effects suffered as a routine operation.

## CONCLUSIONS

The mainly conclusions this work is:

- For the closed system, the inner diameter increase reduces the fume velocity, increasing the boundary layer near walls pipe and reducing the heat transfer for the cooling system;
- For the open system, the temperature increases due to pos combustion all way long the ducts;
- For open system, the entrance air with higher density compresses the hot gases and concentrate the impact areas on the stack;
- CFD show gas analyses after pos combustion very closed with the industry values.

## ACKONWLEDGMENTS

The components of the work thank Lumar Metals Ltda, Arcelor Mittal João Monlevade and Federal University of Minas Gerais (UFMG).

## REFERENCES

1. SHAPIRO, H. N., MORAM, M. J., *Fundamentals of Engineering Thermodynamics*. Ed. New York: John Wiley & Sons; 1988. p.417-435.
2. Innovative Turbulence Modeling: SST Model in ANSYS CFX. TECHNICAL BRIEF ANSYS. [cited 2006 Dec 29]; Available from: <http://www.ansys.com>
3. ANSYS FLUENT “*FLUENT User’s Guide*”, 2005.
4. MALISKA, C. R. *Transferência de Calor e Mecânica dos Fluidos Computacional – Fundamentos e Coordenadas Generalizadas*. ed. LTC – Livros Técnicos e Científicos, 1995, Rio de Janeiro, RJ.
5. Manual do sistema Baunco
6. SCHNELLE, KARL B., BROWN, CHARLES A., *Air Pollution Control Technology Handbook*. Ed. CCR Press, 2001.
7. KERRY, FRANK G., *Industrial Gas Handbook : Gas Separation and Purification*. Ed. CCR Press, 2006.
8. PERRY, ROBERT H., GREEN, DON W., *Perry’s Chemical Engineers Handbook*. Ed. McGaw-Hill, 1997.